Biomimetic Synthesis of Silica Films Directed by Polypeptide Brushes

Jen-Chia Wu,[†,‡] Yuli Wang,[||,⊥] Chia-Chun Chen,*[,‡,§] and Ying-Chih Chang*[,†]

Genomics Research Center, Academia Sinica, Taipei 115, Taiwan, Department of Chemistry, National Taiwan Normal University, Taipei 116, Taiwan, Institute of Atomic and Molecular Science, Academia Sinica, Taipei 106, Taiwan, and Department of Chemical Engineering and Materials Science, University of California, Irvine, California 94027-2575

Received June 28, 2008. Revised Manuscript Received August 1, 2008

Biomimetic porous silica films have been synthesized by polycondensation of tetraethoxysilane on a soft template formed by an "end-tethered poly(L-lysine)" ("t-PLL") monolayer with a brushlike configuration. The silica formation occurs spontaneously inside the t-PLL at neutral pH and room temperature. The growth of silica fully conforms to the original t-PLL film thicknesses and lateral micropatterns, regardless of a prolonged reaction time and the monomer concentration. The morphologies of biomimetic silica are changed from continuous pleated, discrete spherical to fibrous forms according to the initial t-PLL chain length and surface density. After the t-PLL template is burned off, TEM images show the creation of nanochannel arrays in silica with an average diameter of 10 nm. Overall, our approach has provided a straightforward and environmentally friendly route to directly generate silica films with controllable morphology, thickness, and porosity.

Introduction

The biomimetic synthesis of silica materials has progressed significantly in the past few years. The conventional syntheses of silica usually involve elevated temperature, extreme pH, and/or the use of surfactants.[1−5] In contrast, the silicification processes of many biological systems such as diatoms and sponges occur in water at near-neutral pH and ambient temperature. Unlike conventional syntheses, the silicification of the biological systems mostly produces precisely controlled nanostructures and morphologies of the resulting silica materials.[6,7] Recent studies have demonstrated that the biomolecules extracted from biological silica-containing species (e.g., diatoms, sponges) can induce rapid silica precipitation from tetraethyl orthosilicate (TEOS) at ambient conditions in vitro. While these studies suggested that the biomimetic processes are feasible in vitro, the extraction of silica-induction biomolecules required elaborative procedures and yielded only a small quantity of materials. Thus, seeking synthetic materials that can induce silicification in the same manner as biomolecules is an important quest from both industrial and scientific viewpoints. In particular, synthetic polypeptides with abundant available supplies are the most promising candidates for potential applications. Recent studies have shown that some synthetic polypeptides,[8,9] such as poly(L-lysine) (PLL), poly(L-arginine), and diblock copolypeptides[10] (e.g., poly (L-cysteine-*b*-L-lysine)), can form silica precipitates or ordered silica beads by inducing polycondensation of silica from monomeric TEOS or silicic acid at near-neutral pH and ambient temperature. More detailed studies in PLL have shown the effects of its molecular weight and secondary structures on the resulting silica nanostructures. Hawkins et al.[11] first reported that silica synthesized with PLL exhibited different pore sizes correlated with the original α-helical (the formed pore size of the silica is approximately 1.5 nm) or β-sheet (the formed silica has a broad range of pore size, 2−8 nm) structures of PLL molecules. Patwardhan et al.[12] showed that, via a change in the secondary conformation of PLL from α-helical to β-sheet structure, the silica structure shifts from hexagonal plate to spherelike structures. They also showed that the handedness of polylysine does not affect the formation of hexagonal silica. Additionally, many studies

* To whom correspondence should be addressed. E-mail: cjchen@ntnu.edu.tw (C.-C.C.); yingchih@gate.sinica.edu.tw (Y.-C.C.).
† Genomics Research Center, Academia Sinica.
‡ National Taiwan Normal University.
§ Institute of Atomic and Molecular Science, Academia Sinica.
⊥ University of California.
|| Current address: Intellego Co., 7020 Kit Creek Rd., Research Triangle Park, NC 27709.

(1) Brinker, C. J.; Scherer, G. W. *Sol-Gel Science: The Physics and Chemistry of Sol-Gel Processing*; Academic Press: San Diego, 1990.
(2) Zhao, D.; Yang, P.; Melosh, N.; Feng, J.; Chmelka, B. F.; Stucky, G. D. *Adv. Mater.* **1998**, *10*, 1380–1385.
(3) Iler, R. K. *The Chemistry of Silica: Solubility, Polymerization, Colloid and Surface Properties, and Biochemistry*; Wiley: New York, 1979.
(4) Lu, Y.; Ganguli, R.; Drewien, C. A.; Anderson, M. T.; Brinker, C. J.; Gong, W.; Guo, Y.; Soyez, H.; Dunn, B.; Huang, M. H.; Zink, J. I. *Nature* **1997**, *389*, 364–368.
(5) Stober, W.; Fink, A.; Bohn, E. *J. Colloid Interface Sci.* **1968**, *26*, 62–69.
(6) Carole, C. P.; Tracey, K.-T. *J. Biol. Inorg. Chem.* **2000**, *V5*, 537–550.
(7) Mann, S.; Webb, J.; Williams, R. J. P. E. *Biomineralization: Chemical and Biochemical Perspectives*; VCH: Weinheim, Germany, 1989.
(8) Siddharth, V. P.; Niloy, M.; Stephen, J. C. *J. Inorg. Organomet. Polym.* **2001**, *V11*, 193–198.
(9) Coradin, T.; Durupthy, O.; Livage, J. *Langmuir* **2002**, *18*, 2331–2336.
(10) Cha, J. N.; Stucky, G. D.; Morse, D. E.; Deming, T. J. *Nature* **2000**, *403*, 289–292.
(11) Hawkins, K. M.; Wang, S. S. S.; Ford, D. M.; Shantz, D. F. *J. Am. Chem. Soc.* **2004**, *126*, 9112–9119.
(12) Patwardhan, S. V.; Maheshwari, R.; Mukherjee, N.; Kiick, K. L.; Clarson, S. J. *Biomacromolecules* **2006**, *7*, 491–497.

10.1021/cm8017659 CCC: $40.75 © 2008 American Chemical Society
Published on Web 09/23/2008

have been focused on the effects of molecular weight on the formation of silica.[12−15] These studies have demonstrated that silica synthesized by high molecular weight PLL formed hexagonal silica platelets, whereas silica synthesized by low molecular weight PLL formed spherical silica particles.

While the above-mentioned systems were reported in the solution phase, conceivably, development of a preorganized molecular template at a solid interface is of vast technological interest, in that the subsequent silica material assembly at the surface can be greatly simplified. This is especially advantageous for applications such as integrated circuits, optical displays, biochips, etc., where the molecular orientation, surface density, and distribution are of primary manufacturing concerns. Previously, the use of self-assembled monolayers (SAMs) and lithography to form micro- and nanopatterned silica[16−18] (and other inorganic materials[19−25]) at surfaces has been demonstrated, but all required stringent process conditions, such as acid−base catalysis and a high (>100 ppm) and therefore unstable concentration of silicic acid.[26] Even so, the silica structures formed by these routes were still not uniform and controllable, and some collapsed after removal of the template.

Previously, we have shown that a monolayer of an "end-tethered PLL" ("t-PLL") film in a brush configuration can be synthesized by the surface-initiated vapor deposition polymerization (SI-VDP) technique, a surface polymerization conducted in the gas phase in a vacuum.[27] The micropatterns of the t-PLL film are manufacturable on the silicon wafer when combined with photolithography.[28] It is by far the only reproducible method in producing t-PLL films with the widest thickness range on the order of 1−100 nm. In addition, it has been confirmed that, via C-terminal attachment to the amine-functionalized surface, the films are chemically and mechanically stable while undergoing conformational transitions among α-helices, β-sheets, and random coils, induced by external stimuli. In short, the previously established ability to fabricate stable t-PLL surface patterns with precise control of the molecular conformation, orientation, length, and density provides a unique opportunity to conduct biosilicification at surfaces in forming ingrown silica structures with preorganized features such as pore sizes, dimensions, thickness, density, morphology, and nanochannel arrays with tunable diameters and aspect ratios perpendicular to the surface plane.

The surface polycondensation of TEOS templated by t-PLL at neutral pH and ambient temperature was designed and verified by multiple spectroscopic and microscopic techniques. The successful synthesis of t-PLL/silica nanocomposites and the subsequent removal of t-PLL were confirmed by circular dichroism (CD) and Fourier transform infrared (FTIR) spectroscopy. Atomic force microscopy (AFM), scanning electron microscopy (SEM), and transmission electron microscopy (TEM) studies have revealed that the growth of silica films fully conform to the original t-PLL templates in three dimensions. Further controls of the t-PLL density, chain length, and patterns have led to ingrown silica with continuous pleated, spherical, and fibrous forms. The t-PLL films were stable during the surface reaction due to the covalent bonding to the surface. Our results have demonstrated a simple but efficient approach to producing organized biomimetic silica films.

Experimental Section

Cleaning of Substrates. All solid substrates, silicon wafers (Siltec Silicon, single side polished, 500 μm, orientation ⟨100⟩, used in FTIR, ellipsometry, and SEM) and quartz plates (Starna Cells Inc., 45 × 12.5 × 1 mm, used in CD), were cleaned immediately before the surface chemical treatment. The substrates were cleaned with freshly prepared piranha solution (H_2SO_4/H_2O_2 = 7/3 (v/v)) at 120 °C for 40 min. *Caution: The procedure of mixing concentrated sulfuric acid and hydrogen peroxide is highly exothermic, and the piranha solution reacts violently with organic solvents, which will cause an explosion. It should be handled carefully.* After being thoroughly rinsed with deionized water and acetone, the substrates were dried under a stream of nitrogen and immediately used in the silanization step.

Silanization of the Substrates with Various Amine Densities. The silanization procedures were similar to those in previously published papers.[27,29] The substrates were silanized in the (3-aminopropyl)triethoxysilane (APS) vapor phase under reduced pressure for 16 h in a vacuum desiccator. After completion of the reaction, the substrates were removed from the desiccator, ultrasonicated in acetone for 5 min, which was repeated three times, and finally dried under a stream of nitrogen. The characterization of the APS initiator layer followed the previously published methods.[27,29] The film thickness, as determined by ellipsometry, was 8 ± 1 Å (with an assumption of a fixed refractive index of 1.46), indicating full coverage of APS on the surfaces.

We used the stepwise method[30] to prepare surfaces with different amine densities. Chlorodimethylisopropylsilane (CDPS) (0.5%) and [3-(ethoxydimethylsilyl)propyl]amine (EDSA) (1.0%) solutions in anhydrous toluene were prepared. First, cleaned Si wafers were immersed in the CDPS solution for 4, 16, and 24 h to produce various CDPS surface coverages on each sample. The CDPS-modified substrates were then washed with toluene and baked at

(13) Patwardhan, S. V.; Mukherjee, N.; Steinitz-Kannan, M.; Clarson, S. J. *Chem. Commun.* **2003**, 1122–1123.
(14) Rodriguez, F.; Glawe, D. D.; Naik, R. R.; Hallinan, K. P.; Stone, M. O. *Biomacromolecules* **2004**, *5*, 261–265.
(15) Glawe, D. D.; Rodriguez, F.; Stone, M. O.; Naik, R. R. *Langmuir* **2005**, *21*, 717–720.
(16) Brott, L. L.; Naik, R. R.; Pikas, D. J.; Kirkpatrick, S. M.; Tomlin, D. W.; Whitlock, P. W.; Clarson, S. J.; Stone, M. O. *Nature* **2001**, *413*, 291–293.
(17) Coffman, E. A.; Melechko, A. V.; Allison, D. P.; Simpson, M. L.; Doktycz, M. J. *Langmuir* **2004**, *20*, 8431–8436.
(18) Kim, D. J.; Lee, K. B.; Lee, T. G.; Shon, H. K.; Kim, W. J.; Paik, H. J.; Choi, I. S. *Small* **2005**, *1*, 992–996.
(19) Denis, F. A.; Hanarp, P.; Sutherland, D. S.; Dufrene, Y. F. *Langmuir* **2004**, *20*, 9335–9339.
(20) Nakanishi, T.; Masuda, Y.; Koumoto, K. *Chem. Mater.* **2004**, *16*, 3484–3488.
(21) Seo, E. K.; Lee, J. W.; Sung-Suh, H. M.; Sung, M. M. *Chem. Mater.* **2004**, *16*, 1878–1883.
(22) Tokuhisa, H.; Hammond, P. T. *Langmuir* **2004**, *20*, 1436–1441.
(23) Kisailus, D.; Truong, Q.; Amemiya, Y.; Weaver, J. C.; Morse, D. E. *Proc. Natl. Acad. Sci. U.S.A.* **2006**, *103*, 5652–5657.
(24) Tugulu, S.; Harms, M.; Fricke, M.; Volkmer, D.; Klok, H. A. *Angew. Chem., Int. Ed.* **2006**, *45*, 7458–7461.
(25) Yang, P.; Yang, M.; Zou, S.; Xie, J.; Yang, W. *J. Am. Chem. Soc.*, in press.
(26) Patwardhan, S. V.; Clarson, S. J.; Perry, C. C. *Chem. Commun.* **2005**, 1113–1121.
(27) Wang, Y.; Chang, Y. C. *Macromolecules* **2003**, *36*, 6511–6518.
(28) Wang, Y.; Chang, Y. C. *Adv. Mater.* **2003**, *15*, 290–293.
(29) Wang, Y.; Chang, Y. C. *Langmuir* **2002**, *18*, 9859–9866.
(30) Choi, I.; Kim, Y.; Kang, S. K.; Lee, J.; Yi, J. *Langmuir* **2006**, *22*, 4885–4889.

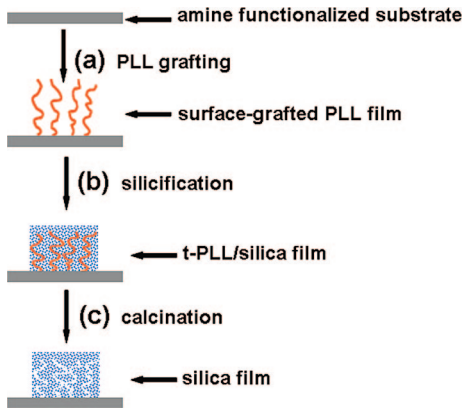

Figure 1. Schematic illustration of the hypothesized process of the biomimetic silicification induced by a surface-grafted poly(L-lysine) (t-PLL) monolayer: (a) t-PLL brushes in distilled water, (b) silicification at neutral pH and room temperature, (c) calcination at 450 °C for 4 h to burn off the t-PLL template.

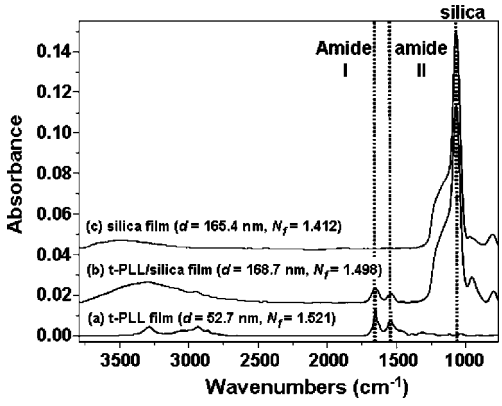

Figure 2. FTIR spectrum of a t-PLL film on a silicon wafer, followed by (a) 24 h silicification and (b) 4 h calcination at 450 °C. The proposed structures of the corresponding films are illustrated in Figure 1. The film thickness (d) and refractive index (N_f) of each dry film are labeled above the corresponding FTIR spectrum.

120 °C for 30 min, followed by the second immersion in the EDSA solution for 24 h to saturate the surface-bound silane layer. The substrates then were cleaned with toluene and baked at 120 °C for 30 min. Finally, the CDPS/EDSA-modified substrates were sonicated in toluene, acetone, and ethanol sequentially to thoroughly remove loosely bound physisorbed materials.

Synthesis of t-PLL Films. The fabrication of t-PLL films on the amine-modified planar solid substrates followed the previously published procedures with minor modification.[27,29] End-tethered poly(N^{ε}-carbobenzyloxy-L-lysine) (t-PCBL), the precursor of t-PLL, was grown from the amine-modified (APS or EDSA) solid substrates by SI-VDP of the *N*-carboxyanhydride (NCA) of N^{ε}-carbobenzyloxy-L-lysine (CBL) at a 102 °C substrate temperature, the NCA evaporation temperature, and 1.0×10^{-5}−1.0×10^{-6} Torr with a 1 h reaction time for the samples used in Figures 2−7 and the thicker t-PLL films used in Figure 10a−c or a 40 min reaction time for the thinner t-PLL films used in Figure 10d−f. After the SI-VDP reaction was completed, the samples were sonicated in a mixture of dichloroacetic acid (DCA)/chloroform (2/8, v/v) for 5 min, washed with chloroform, and dried under a stream of nitrogen. To remove the N^{ε}-carbobenzyloxy protecting groups of t-PCBL, the samples were suspended in the benzene layer of the hydrogen bromide/benzene mixture (2/8, v/v) and sonicated for 40 min, followed by successive rinses with toluene, acetone, and distilled water, and then dried under a stream of nitrogen, yielding t-PLL films.

To create t-PLL surface patterns, SI-VDP and photolithography were combined, followed by the previously published method with minor modification.[28] The 10 μm stripes and 10 μm intervals between the stripes were fabricated, suitable for the studies under AFM. A 1 mm stripe was also fabricated on the same substrate next to the micropatterned area, suitable for the ellipsometry measurements.

Surface-Grafted Polypeptide-Templated Synthesis of Silica. The t-PLL-bound substrates were fixed on the bottom of a Petri dish or an ellispometer liquid cell (Gaertner Inc.). A 60 mL portion of distilled water (pH 6.86) was added to the cells, followed by the addition of 0.12 mL of TEOS. The TEOS and water are immiscible, with the TEOS layer on top of the water layer. According to the definition of "immiscible" (the solubility of the solute is under 1.0×10^{-4} M), the concentration of the silicic species in our system would be very low and close to that of the oceans (ca. 70 μM).[26,31] This configuration design provides a very stable TEOS concentration in the water phase during the silicification reaction. The TEOS layer was gradually hydrolyzed and provided a steady source of silicic acid for silicification. In our case, the distance between the TEOS−water boundary and the t-PLL film surface was about 2 cm. The cells were opened to exposure to the atmosphere (temperature 25 °C, relative humidity 60%) throughout the silicification reaction. After the completion of silicification, the substrates were taken out of the Petri dish or liquid cell, rinsed with acetone and distilled water, and dried under a stream of nitrogen. For all of the samples in this paper, a silicification time of 12 h was used, which was the time required for the thickest sample to finish the silicification reaction.

Calcination of Surface Silica. To remove the t-PLL template of the t-PLL/silica films, the samples were calcinated in air by being heated on a digitally controlled chemical vapor deposition (CVD) system (Lindberg/Blue-M) for 4 h at 450 °C, with an initial heating rate of 100 °C/min.

Instrumentation. FTIR spectra of the t-PLL films, t-PLL/silica films, and calcined silica films (on the silicon substrates) were recorded using a Nicolet Magna-IR 860 spectrometer in transmission mode with a clean silicon wafer as the reference. The sample collection parameters were 32 scans and resolution 4 cm^{-1} for all the samples. The spectral measurements were performed under dry air (Whatman FT-IR purge gas generator) purging to offset absorption of moisture.

Ellipsometric measurements of the films on silicon wafers, in both air and solutions, were performed with a Gaertner LSE Stokes ellipsometer with a He−Ne laser (λ = 632.8 nm) and a fixed incident angle of 70°. The film thicknesses were measured after each preparation step. After piranha solution cleaning and APS modification, the substrates were measured to find the N_s (3.85), K_s (−0.02), and refractive index (1.00) of the ambient. The refractive indices of the ultrathin layer of the native silicon oxide layer on the substrates and the APS layer were fixed to 1.46. In the cases of the dry t-PCBL and t-PLL films, the refractive indices of the films were automatically calculated by the Gaertner ellipsometer measurement program. To measure the solvated t-PLL films at the solid−water interface, a custom liquid cell[32] was used, and the refractive index of the aqueous phase (distilled water and buffer solutions) was simply set to 1.333. The final thicknesses of the t-PLL films were obtained by subtracting the thickness of the oxide layer (17.8 Å) and APS (8 Å) from the calculated thickness. All the measurements of the thickness and refractive index of the

(31) Treguer, P.; Nelson, D. M.; Van Bennekom, A. J.; DeMaster, D. J.; Leynaert, A.; Queguiner, B. *Science* **1995**, *268*, 375–379.
(32) Wang, Y.; Chang, Y. C. *Macromolecules* **2003**, *36*, 6503–6510.

samples were performed at least three times with random locations on each sample.

CD (JASCO J-60 spectropolarimeter) was used to examine the conformation of t-PLL on quartz, for both t-PLL and t-PLL/silica films in pH 7 and 9.5 buffers (5 mM bis-tris-propane), respectively. A rectangular demountable liquid cell (Starna Cells Inc.) with a 1 mm path length was used. To fix the quartz plate to the liquid cell, a cell holder was used, as described previously.[32] Three separate spectra were recorded at a band width of 1 nm and a scanning rate of 20 nm/min.

All of the SEM images were inspected by using a JEOL-JSM-6700F scanning electron microscope, with a platinum coating. To take the cross-sectional SEM image, a custom sample holder with a 1 cm depth groove was used, and the substrate was tilted vertically and stuck on the side wall of the groove.

AFM images of the patterned t-PLL film, t-PLL/silica film, and calcined silica film were obtained with an Asylum Research MFP-3D atomic force micrscope operated in the tapping mode with an Al-300 cantilever (Olympus). The image of the patterned t-PLL film in distilled water was obtained by using a biocantilever (Olympus).

A goniometer (FDS-OCA15 plus) was used to measure water contact angles at solid−liquid interfaces. The droplets used were 3 μL, and the measurements were performed at least three times with random locations on each sample.

The TEM images were acquired with a JEOL-JEM-2100F transmission electron microscope at high voltage (150 kV). The sample used for taking the TEM cross-section image required additional preparations. Seven wafer pieces, each 1 cm in width and 0.5 cm in length, were fixed to the substrate, with four pieces fixed with the polished side facing the sample layer of the substrate and the other three pieces with the polished side facing the back of the substrate. Both sides of the substrate were polished until the sample was penetrable by light. Then the filmlike sample was mounted on a Cu ring and removed from the polish holder. Finally, the film fixed in the Cu ring was polished by a precision ion polishing system to make the sample thin enough to image with the transmission electron microscope.

Results and Discussion

In Situ Synthesis of Silica Nanostructures at Solid Surfaces. The procedure for the direct synthesis of silica at surfaces can be separated into three preparation steps: the preparation of an amino-functionalized surface by silanization of silicon oxide based surfaces, the formation of t-PLL films by SI-VDP of CBL, and then the deprotection of the side chains of t-PCBL (Figure 1a).[27,29] The amino acid monomer, CBL, was heated at 102 °C in a vacuum to generate the monomer vapor, which was readily polymerized through the ring-opening surface polymerization when in contact with the immobilized surface APS initiators or N-terminated propagated peptide chains. The so-called SI-VDP process has been shown to produce consistent results previously in multiple amino acid systems, with the highest thickness of end-tethered polypeptide films reported by far.[27,29,32,33] By changing the reaction parameters such as the reaction time, temperature, and vacuum pressure, the resulting polypeptide film thickness could be varied from a few nanometers to submicrometers, translating to tens to thousands of repeating amino acids in one chain.[27,29,32,33] The ability to produce multiple lengths of surface-grafting polypeptides with great chemical stability was the key to successfully producing biomimetic silica. Previously, the surface properties of t-PLL films in both ambient and aqueous environments have been carefully characterized on the basis of the measurements from ellipsometry, FTIR, CD, and a quartz crystal microbalance with dissipation. In neutral pH solutions (buffer or water), the t-PLL chains were fully stretched away from the surface, adopting an extended randomly coiled conformation as a result of their highly charged amino side chains at neutral pH. In contrast to dry t-PLL films in which the t-PLL chains interweave and collapse, the solvated, preferentially upright randomly coiled t-PLL chains in neutral pH are more likely to provide an accessible interchain space for silica penetration. Here, the t-PLL-bound substrates were fully immersed in the aqueous phase of the distilled water (bottom layer)/TEOS (top layer) immisible solutions. The TEOS diffused to the water phase. At thermodynamic equilibrium, this design provides a constant TEOS concentration in the water phase. At neutral pH, TEOS was gradually hydrolyzed into anionic silica species. The solvated, cationic t-PLL random coil brushes may serve as the adsorption center to attract TEOS in close proximity for polycondensation to take place, thus forming a t-PLL/silica nanocomposite film (Figure 1b). To create a pure silica porous structure, the nanocomposite can be calcined at high temperature (450 °C) in ambient conditions to remove the t-PLL template (Figure 1c).

As a blank control, a silicon wafer without a t-PLL film was placed in the water/TEOS solution for several days, and we found no silica precipitation or silica deposition on the clean silicon wafers, as examined by ellipsometry and FTIR. When t-PLL-modified substrates were introduced, however, a spontaneous silicification was induced, as confirmed by the resulting FTIR spectra (Figure 2). For the t-PLL film on the silicon wafer prior to the silicification reactions (Figure 2a), the distinct IR peaks at 1652 cm^{-1} (amide I) and 1544 cm^{-1} (amide II) were attributed to the characteristic peaks of PLL. It is noted that, although typically there is an about 18 Å native silicon oxide layer on the silicon substrate, the use of a clean silicon substrate as the background spectrum when the IR absorbance spectrum was taken resulted in no observable absorption peak around 1069 cm^{-1}, the characteristic Si−O−Si stretching absorption for silica. After 24 h of immersion in the water/TEOS solution, a strong absorption at 1069 cm^{-1} appeared, suggesting silica formation (Figure 2b). The broader peak width of both amide I and amide II suggested a change in the environment surrounding the t-PLL chains. The broad band around 3300 cm^{-1} was assigned to water absorption. After 4 h of heating at 450 °C, the t-PLL template was shown to be removed, yielding a pure silica film, with the disappearance of the amide I and the amide II absorption peaks altogether (Figure 2c). In the FTIR spectrum of the calcified silica, the broadened peak centered around 3500 cm^{-1} corresponded to the presence of silanol groups (Si−OH), indicating an incompletely polymerized silica network. The partially polymerized silica network was characteristic of the silica found in biological materials.[6,12,34,35]

(33) Lee, N. H.; Frank, C. W. *Langmuir* **2003**, *19*, 1295–1303.

(34) Frohlich, F. *Terra Nova* **1989**, *1*, 267–273.

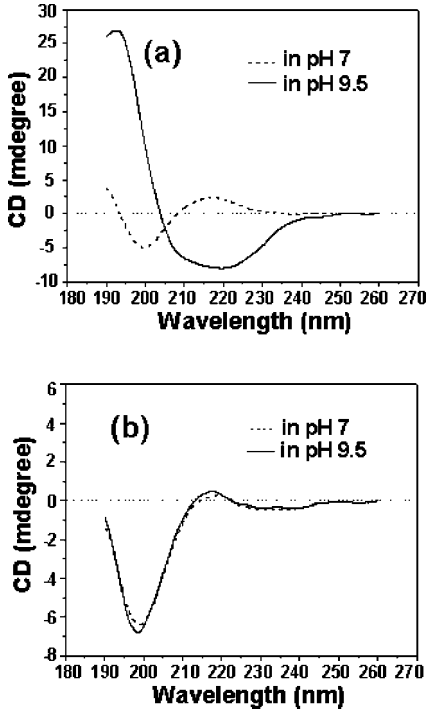

Figure 3. CD spectra of (a) a t-PLL film and (b) a t-PLL/silica film in pH 7 and 9.5 buffers (5 mM bis-tris-propane). Quartz substrates were used.

The FTIR spectrum, thickness (d), and refractive index (N_f) of each dry film are shown in Figure 2. In the dry t-PLL film, the t-PLL molecular chains were tilted toward the surface, giving a 52.7 nm thick film with a relatively compact structure ($N_f = 1.521$). When the t-PLL film was immersed in neutral distilled water, the t-PLL molecular chains were solvated and brushlike,[29] increasing the film thickness to 163.5 nm. More significantly, after the completion of silicification, the t-PLL/silica film had a thickness of 168.7 nm, which was comparable to the original thickness of the solvated t-PLL film. The calcination of the t-PLL/silica film at 450 °C burned off the PLL molecules, resulting in a porous silica film, as evidenced by the decrease of N_f from 1.498 to 1.412, while the film thickness remained approximately identical. The calcined film should have a high aspect ratio, threadlike porous structure as illustrated in Figure 1, as the imprint of the original presence of t-PLL molecular chains. This will be further demonstrated in the high-resolution TEM image.

Molecular Chain Mobility Studied by CD. The chain conformation of t-PLL before and after silicification could be characterized by CD spectroscopy because silica had no absorption in the detected ultraviolet light range (190−260 nm). It is known that the conformations of solvated t-PLL can be interconverted by pH: at neutral or acidic pH, t-PLL adopts a randomly coiled structure, while at pH 9.5, it adopts an α-helical structure (Figure 3a).[27] However, in the t-PLL/silica film, the t-PLL molecular chains were embedded inside the silica. The chains thereby lose the flexibility to interconvert conformations, adopting only the randomly coiled structure, even in a basic buffer at pH 9.5 (Figure 3b). This result confirmed the proposed structure of the t-PLL/silica film shown in Figure 1, in which the embedded randomly coiled t-PLL molecular chains are fixed by silicification.

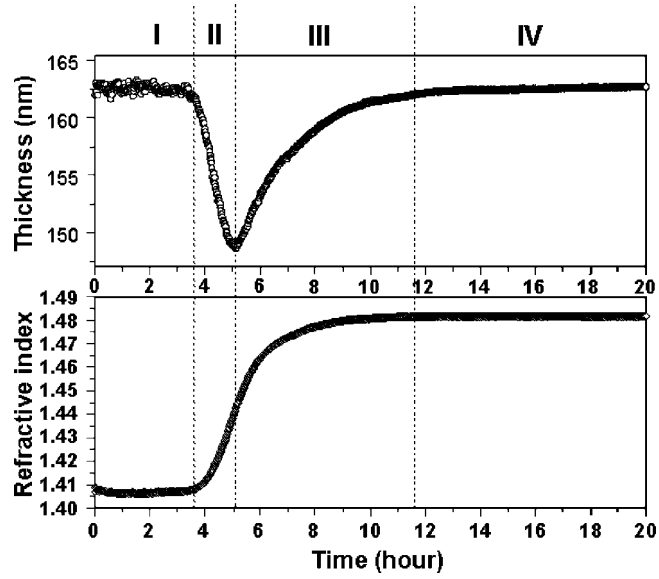

Figure 4. Thickness and refractive index (in water) in the course of silicification induced by a t-PLL film monitored by in situ ellipsometry. The progress can be divided into four regions. Step I is the induction region, in which no silica is formed. In step II, silica begins to form around the t-PLL molecular chains and causes shrinkage of the film thickness and an increase of the refractive index. Step III is the further growth step, which causes an increase of the film thickness and refractive index. After all the space around the t-PLL molecular chains is occupied, silicification is stopped (step IV).

Silica Growth Monitored by in Situ Ellipsometry. In situ ellipsometry, which can monitor the film thickness and refractive index in a liquid, gave direct observation of silica growth. Figure 4 shows the changes of the thickness and refractive index during the silicification process. This process can be divided into four Steps. Step I is the induction region, in which the concentration of silica anionic species (hydrolyzed from TEOS) is so low that no silica is formed. This was confirmed by the lack of visible silica when analyzed by SEM (data not shown). We noted that the ellipsometry curve in this step was not very stable and may experience fluctuation between different sets of experiments. When the silica anionic species are accumulated to a certain concentration, silica begins to form around the t-PLL molecular chains. Due to the gravity and charge neutralization, the t-PLL molecular chains start to shrink and collapse toward the surface, causing shrinkage of the film thickness and an increase of the refractive index (step II). As more and more silica is filled, the t-PLL molecular chains become fixed, and the film thickness stops decreasing. Futher growth of the silica causes an increase of the film thickness, with the refractive index continouesly increasing (step III). After all the space around the t-PLL molecular chains is occupied, silicification is stopped (step IV). In this particular case, it takes approximately 12 h to complete the silicification process. Overall, the fill of silica into the t-PLL film caused the refractive index to increase from 1.408 to 1.481 (in distilled water). The t-PLL/silica film (∼162 nm, in distilled water) had almost the same thickness as the t-PLL film (∼163 nm, in distilled water), indicating that the silicification only conformed to the t-PLL film. Therefore, the growth of

(35) Parkinson, J.; Gordon, R. *Trends Biotechnol.* **1999**, *17*, 190–196.

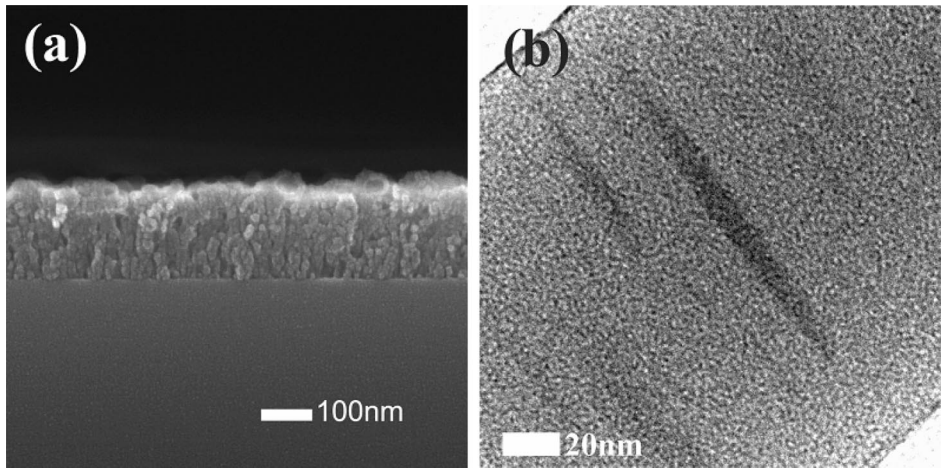

Figure 5. (a) SEM (scale bar 100 nm) and (b) TEM (scale bar 20 nm) images of the cross-section of the silica film.

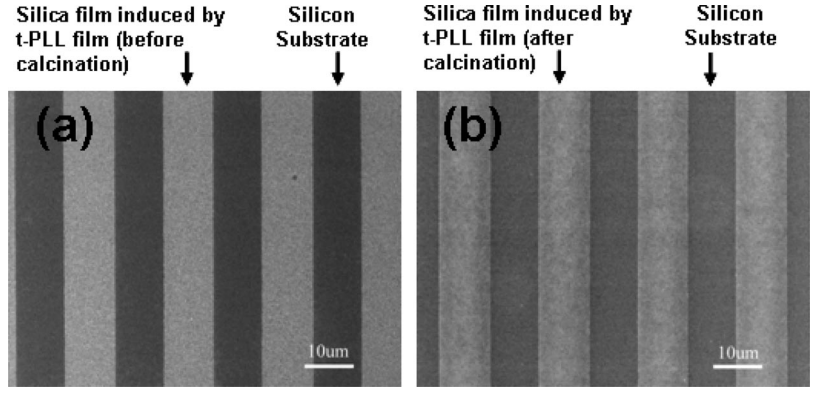

Figure 6. SEM images of (a) the micropatterned t-PLL/silica film and (b) the calcined silica film induced by the patterned t-PLL film (the patterned stripes are 10 μm, and the intervals are 10 μm). The arrows and captions above the SEM images describe the composition differences between the white and black strips. The white strips are the t-PLL/silica hybrid film in the SEM image in (a) and the silica film only in the SEM image in (b). The black strips are bare silicon substrate in the SEM images in both (a) and (b).

silica is completely directed by t-PLL in the vertical direction. The film thickness of t-PLL can be controlled by the reaction time during the SI-VDP reaction, ranging from a few nanometers to hundreds of nanometers, with an accuracy within 10 nm.[27] Therefore, the thickness of the synthesized silica film can be easily tuned by varying the thickness of the t-PLL film (data not shown).

SEM and TEM images, shown in Figure 5, further revealed the nanostructures of the t-PLL/silica films. The cross-sectional SEM image confirmed the thickness of silica, which was consistent with the ellipsometric measurements. The silica granular structures appeared to be grouped along the surface normal (Figure 5a). The randomly selected cross-sectional TEM image further revealed the distinct electron density distribution (Figure 5b). The darker, parallel stripes suggested preferentially unidirectional cylindrical pores (around 5−15 nm in diameter) inside the silica film, and the aspect ratios of the nanosize channels ranged from 10 to 30. According to Daniel et al.,[11] the silica synthesized with solvated PLL in an α-helix conformation possesses cylindrical pores of approximately 1.5 nm diameter, whereas silica synthesized with PLL in a β-sheet conformation possesses larger pores with a broad range (2−8 nm) of pore sizes (the size being a function of the PLL concentration, or in other words the size of the aggregates). Unlike those results, our silica films were synthesized with t-PLL in a randomly coiled structure, and the formed pore size was in the range of 5−15 nm. The larger pore size and the broader pore size distribution are likely due to the randomly coiled secondary structure in the t-PLL films we used as well as the aggregation of the t-PLL molecular chains. Furthermore, it deserves mentioning, as we know, the chain length of the t-PLL can be controlled by the reaction time of SI-VDP (with a range of 1−250 nm in length in the distilled water or buffer solution); by the control of the chain length and structure of the t-PLL, the aspect ratio of the nanochannels could be modulated easily in a wide range (around 50−0.06).

Formation of Patterned Silica Films. Because silicification is templated by the t-PLL film, a micropatterned silica film can be predetermined by a patterned t-PLL film. In our work, the patterned t-PLL film served as the template to organize the deposition of silica. Figure 6 shows the SEM images of a micropatterned t-PLL/silica film and the calcined silica film induced by the patterned t-PLL film. In the regions absent of t-PLL, the surface was clean and no formation of silica was observed. Silica can be formed only in the regions where t-PLL is present. Thus, the silicification can be templated by the t-PLL film in lateral directions, with precision on the order of 5 nm. The silica film shown in Figure 6b was calcined at 450 °C in the thermal CVD system, and the resulting silica film was smooth and crack-free, with the silica film bonding to the substrate very firmly. To

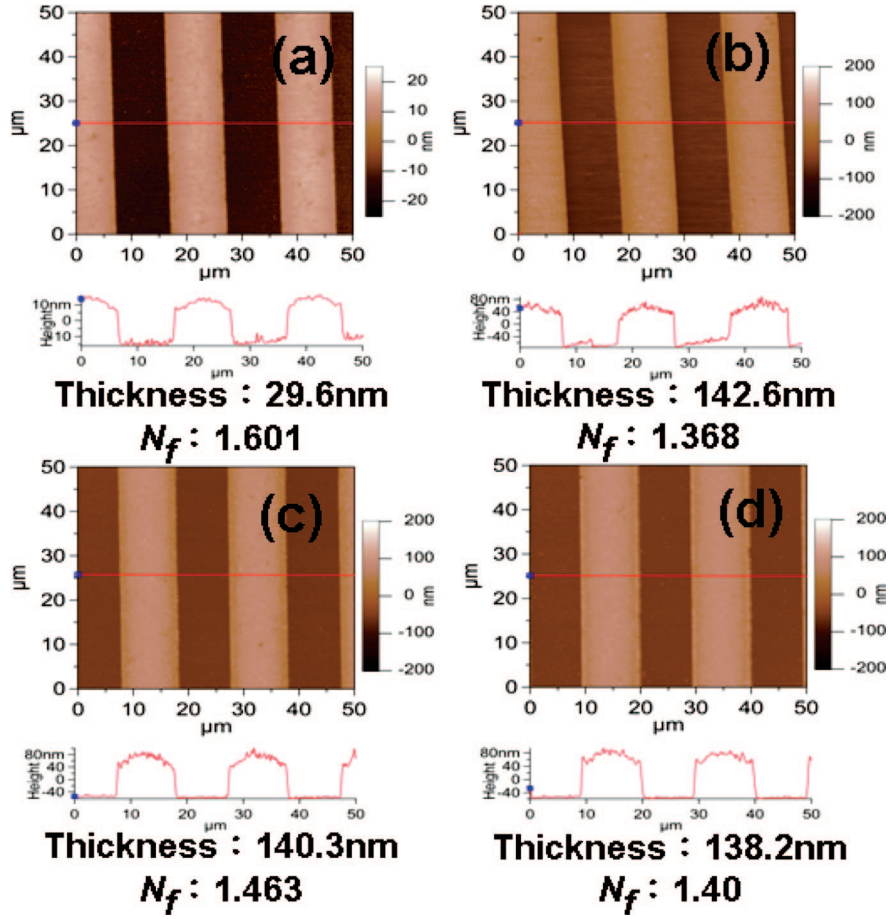

Figure 7. AFM images of the micropatterned (a) surface-grafted t-PLL film in air, (b) surface-grafted t-PLL film in distilled water, (c) t-PLL/silica film, and (d) silica film (scan area 50 μm × 50 μm). The thickness and N_f values shown under the AFM images were measured by optical ellipsometry.

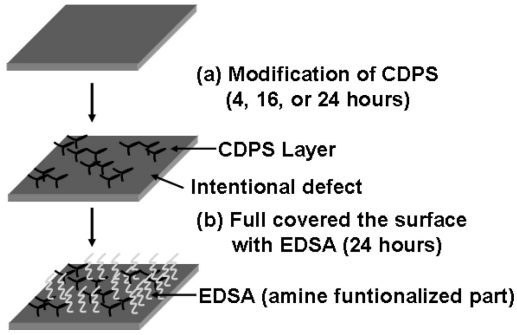

Figure 8. Schematic illustration of the surface modification processes: (a) modification of CDPS, which produces intentional defects on the surface, (b) full coverage of the surface with EDSA.

confirm the ellipsometry data, we analyzed the film thickness data of the patterned film in three steps of silica growth by both optical ellipsometry and AFM (Figure 7). From the comparison of the data collected by optical ellipsometry and AFM in Figure 7, we can see that the thicknesses of the patterned t-PLL film (in air and distilled water), t-PLL/silica film, and silica film were approximately the same in AFM scans. The AFM data reconfirm that the ellipsometry-generated data are authentic.

Binary Silane Treated Surface. Since the silica film bonds to the substrate very firmly, we attempted to alter the surface density of t-PLL to determine the density effects on the silicification reaction and the resulting silica structure. We used the stepwise method[30] to prepare surfaces with

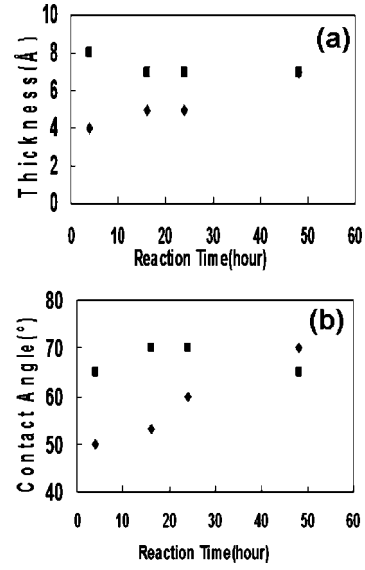

Figure 9. Water contact angle (a) and thickness (b) measurements as a function of time for different amine density surfaces (◆) surfaces modified with CDPS only, (■) surfaces modified with CDPS and then full coverage of the intentionally formed defects with EDSA.

lower amine density, which in turn reduced the surface initiation sites during the SI-VDP process. Briefly, the method deliberately produces intentional defects by first immersing the clean silicon substrate in the CDPS (0.5%) in anhydrous toluene solution for 4, 16, 24, and 48 h, respectively, followed by a second immersion in EDSA

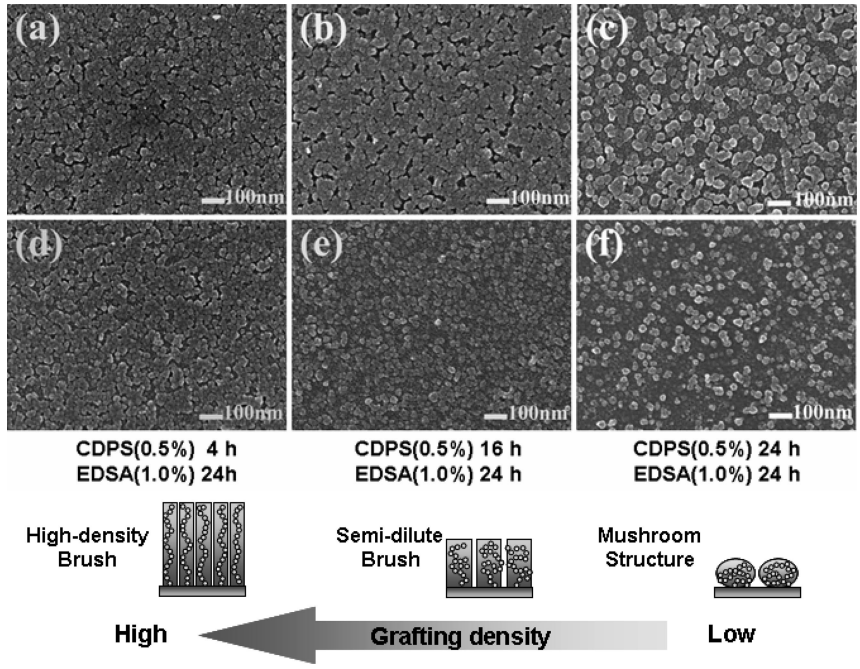

Figure 10. Morphologies of silica synthesized with different densities of t-PLL films on the surface. (a) and (d), (b) and (e), and (c) and (f) are the substrates that were modified by being immersed in 0.5% CDPS toluene solution for 4,16, and 24 h, and then full coverage of the intentionally formed defects of the surfaces was obtained by immersion in 1.0% EDSA toluene solution for 24 h. The thickness of the t-PLL films in (a)−(c) is ∼70 nm and that of the films in (d)−(f) is ∼45 nm in distilled water. The diagram under the SEM images is the proposed model that describes the structure change when the grafting density of the polymer chains is changed.

(1.0%) solutions to fill the remaining space (Figure 8) with amine initiators. The contact angle gradually rises with increased CDPS immersion time (Figure 9a), indicating effectively changing CDPS coverage. It is noted that, in this set of experiments, the monosilanes were used to prevent self-polymerization to guarantee that the functionalized parts would not be overgrown. The diluted amine-modified substrates were then used followed by the same procedure to produce t-PLL and subsequent silica-modified surfaces.

Ellipsometry was used to measure the resulting film thickness of the t-PLL film. In Figure 10a−c, where the surfaces were pretreated with 0.5% CDPS for 4, 16, 24 h, the thicknesses of dry t-PLL films are 12.7, 10.5, and 9.6 nm, and their corresponding thicknesses in water are 78.1, 71.9, and 70.1 nm. The dramatic thickness differences between dry (neutral, collapsed) and wet (charged, fully stretched) films indicate successful dilution of the t-PLL molecular chains at the surfaces.

Influences of the Grafting Density and Molecular Weight of t-PLL on Silicification. Using the diluted t-PLL film as the template, we can observe that the silica distribution was gradually separated by the reduced density of t-PLL on the surface, as shown by the SEM images in Figures 10a−c. This further proves to us that the silica formation was specifically directed by t-PLL. Unlike the previous silica samples, where the final thickness and lateral patterns fully conform to the t-PLL films' original thickness and patterns, in the diluted t-PLL films, the thickness of the t-PLL/silica films changed to 38.9, 21.0, and 19.8 nm, respectively. From the SEM images in Figure 10a−c, we can see that the structure of the t-PLL/silica films shifted from more of a continuous film to silica spheres. The changes in the silica structure morphologies and the thickness of the films might be due to the t-PLL molecular chains being separated by the surface treatment, providing more free space for the t-PLL molecular chains to fold, such that the silica structures preferred to form silica spheres, leading to thickness reduction. These results are similar to the model (the diagrams are shown under the SEM images of Figure 10) proposed by Advincula et al. previously.[36−39] The proposed models are based on the grafting density of the polymer chains. If the distance between two anchoring sites were large, the polymer chain would favor formation of a mushroom structure, which is similar to our lowest grafting density case that directs the formation of the spherelike silica structure. When the grafting density is raised, the distances between the anchored polymers is shortened and the segments of the chains avoid each other as much as possible and minimize segment−segment interactions by stretching away from the surface to form semidilute and high-density brushes. In our cases, the directed silica structure forms a thicker and more continuous silica film as the grafting density is raised. The proposed model quite conforms to the results we get here.

We also tested the influence of the molecular weight. The SEM images of t-PLL/silica films that were synthesized with longer t-PLL molecular chains (∼70 nm, in distilled water)

(36) Degennes, P. G. *J. Phys. (Paris)* **1976**, *37*, 1445–1452.
(37) Fleer, G. J.; Cohen Stuart, M. A.; Scheutjens, J. M. H. M.; Cosgrove, T.; Vincent, B. *Polymers at Interfaces*; Chapman & Hall: London, 1993.
(38) Jones, R. A. L.; Richard, R. W. *Polymers at Surfaces and Interfaces*; Cambridge University Press: Cambridge, U.K., 1999.
(39) Advincula, R. C.; Brittain, W. J.; Caster, K. C.; Ruhe, J. *Polymer Brushes: Synthesis, Characterization, Applications*; Wiley-VCH: Weinheim, Germany, 2004.

are shown in Figure 10a−c, and the SEM images of t-PLL/silica films that were synthesized with shorter t-PLL molecular chains (∼40 nm, in distilled water) are shown in Figure 10d−f. The results of Figure 10d−f were similar to those of Figure 10a−c in that the silica structures were gradually separated to a more loose structure and the t-PLL/silica films were thinner than the t-PLL films in water. In comparison with the samples in Figure 10a−c, it was readily apparent that silica synthesized with the lower molecular weight t-PLL resulted in the formation of smaller silica spheres.

In addition to PLL, other surface-grafted polypeptides were tested with different side groups, such as poly(L-glutamic acid) (PLGA) with anionic carboxylic acid groups, poly(L-ornithine) (PLO) with cationic amino groups, and poly(L-phenylalanine) (PLPA) with un-ionized groups. There was no trace of silica formed in the PLGA and PLPA films, while silicification can be induced by PLO as it was by PLL. These results suggest that the positively charged side groups (e.g., NH_3^+) are responsible for the silicification. These groups can provide nucleation sites, which bring the negatively charged silica oligomers close enough for polycondensation to occur.[9] Because the negatively charged side groups (COO^-) seem to inhibit the silica formation, by carefully designing the structure of surface-grafted polypeptides (e.g., PLGA-*b*-PLL block copolypeptide),[40] silica films with complicated structures might be fabricated.

Conclusions

In summary, inspired by biomimetic silicification in solutions, this study introduces a mild and environmentally benign approach to synthesize silica films at the solid−water interface by using a t-PLL film as a template. The first innovation of this approach is the mild reaction condition, combining a neutral pH condition, ambient temperature, and the absence of any surfactants. This is in contrast to the sol−gel approach to synthesize mesoporous silica films on a solid support, in which acidic conditions and surfactants are essential.[41] The second innovation is that the synthesized silica films are mediated by the t-PLL films both chemically and geometrically, making accurately patterned silica possible. Furthermore, in the experiments that combined the surface-grafted technique with binary silanes, we further demonstrate that the silica structure could be accurately controlled by modulating the t-PLL film (such as changing the grafting density of t-PLL or the molecular weight of t-PLL). The research here is helpful for us to better understand the role of PLL in controlling silica formation, and the techniques might be applied to synthesize other materials and in further applications.

Acknowledgment. This work was supported in part by a grant from the National Taiwan Normal University and Genomics Research Center and Institute of Atomic and Molecular Science at Academia Sinica. We also thank Hung-Chun Lo and Yi-Cheng Lee for their help with SEM and TEM imaging.

CM8017659

(40) Pender, M. J.; Sowards, L. A.; Hartgerink, J. D.; Stone, M. O.; Naik, R. R. *Nano Lett.* **2006**, *6*, 40–44.

(41) Sugimura, H.; Hozumi, A.; Kameyama, T.; Takai, O. *Adv. Mater.* **2001**, *13*, 667–670.